GEOPHYSICAL RESEARCH LETTERS, VOL. 25, NO.16, PAGES 3103-3106, AUGUST 15, 1998

Natural electromagnetic pulses in the ELF range

Alexander P. Nickolaenko[1] and Masashi Hayakawa

Department of Electronic Engineering, University of Electro-Communications, Chofu, Tokyo, Japan

Abstract. We analyze the propagation of electromagnetic waves in the ELF. We apply the modal solution for the spherical Earth–ionosphere cavity and obtain the time domain fields using the FFT algorithm. The Schumann resonance amplitude over the frequency–distance plane consists of summits and depressions exhibiting separate extended zones. When the source–observer distance is small, the field maximum is found at some hundred hertz. This component rapidly decays with the distance. The time domain ELF pulse travels with a constant velocity and "bounces" from the source antipode. Its width increases along the path due to absorption of the high frequency component. The distance dependence of the pulse amplitude depends on both the geometrical focusing and the high frequency absorption.

1. Introduction

An interest to the monitoring of the natural pulsed radio signals re-appeared recently, stimulated by the attempts to locate the distant powerful lightning strokes that cause optical emissions in the upper atmosphere [see *Lyons,* 1994; *Sentman and Westcott,* 1993; *Sentman et al.,* 1995 and references therein]. The observations were performed over the USA territory, and the position of causative strokes was established with the National Lightning Detection Network. To cover a wider territory, an application of the Schumann resonance had been suggested that occupies frequencies from a few to some tens of hertz [*Boccippio et al.,* 1995]. The slow-tail technique is applied as a rule at distances of a few thousand km [see *Wait,* 1962; *Reising et al.,* 1996; *Sukhorukov and Stubbe,* 1997 and references therein]. Slow-tails are observed in the frequency range from a few hundred to a few thousand Hz. Neither of the techniques is new: they were developed and used actively during 60s–70s [*Ogawa et al.,* 1967; *Kemp and Jones,* 1971]. The zero-order mode, or TEM wave propagates in the Earth-ionosphere waveguide at frequencies below 1.6–1.7 kHz. The first transverse resonance occurs at the above frequency [*Nickolaenko and Rafalsky,* 1983, *Hayakawa et al.,* 1994] having the particular value that depends on the day- or night-time propagation conditions. Higher-order modes appear at frequencies above the first transverse resonance.

The wave attenuation factor is small below 100 Hz frequency, and the radio wave travels around the Earth. The wave attenuation grows with frequency, the the round-the-world signal becomes too small, and the Schumann resonances vanish:the spectra become uniform. Probably, this spectral difference was one of the reasons why the Q-bursts in the SR range and the slow-tails were traditionally treated separately.

The goal of our study is an analysis of the EM solution within the whole ELF band. We apply the modal representation for the waves in the spherical Earth-ionosphere cavity in frequency domain. The numerical Fourier transform of the spectra provides the time dependent fields. Within such an approach, no modification of the known theory proves necessary, and we compute the fields over the frequency–distance plane from a unique stand.

2. Model

We describe the ELF electromagnetic wave using the modal representation [*Wait,* 1962, *Galejs,* 1972]:

$$E_r(\omega) = \frac{i\nu\,(\nu+1)}{\omega}\,\frac{M_c(\omega)}{4ha^2\varepsilon}\,\frac{P_\nu\,[\cos(\pi-\theta)]}{\sin\pi\nu} \qquad (1)$$

$$H_\varphi(\omega) = -\frac{M_c(\omega)}{4ha}\,\frac{P_\nu^1[\cos(\pi-\theta)}{\sin\pi\nu} \qquad (2)$$

We use the spherical coordinate system (r,θ,φ) with the origin at the center of the Earth, the source and observer are placed in the points $(r_s = a;\theta_s = 0;\varphi_s = 0)$ and $(r_o = a;\theta_o = \theta;\varphi_o = 0)$ correspondingly. The spectral components of the field are in $V\ sec\ m^{-1}$ and $A\ sec\ m^{-1}$; $\nu(\omega)$ is the dimensionless propagation constant of the radio wave; ω is the circular frequency; $M_c(\omega) = const = 10^8 A\ m\ s$ is the current moment of the source; θ is the angular distance between the source and observer; $a = 6.4\ Mm$ is the Earth's radius; $h = 60\ km$ is the effective height of the ionosphere in meters; ε is the dielectric constant of the free space; $P_\nu(x)$ and $P_\nu^1(x)$ are the Legendre and associated Legendre functions; the time dependence is $\exp(+i\omega t)$.

[1]On leave from the Institute of Radiophysics and Electronics, Ukrainian National Academy of Sciences, Kharkov, Ukraine.

Paper number 98GL01699.
0094-8534/98/98GL-01699$05.00

Since $M_c(\omega) = const$, its Fourier conjugate in the time-domain is a Dirac's delta–pulse. The single zero-order mode, or TEM wave propagates in the range from a few hertz to approximately 2 kilohertz.

One has to introduce an appropriate $\nu(f)$ dependence before computing the fields. The problem is in the rarity of the wide–band experimental data at the ELF frequencies, [see e.g. *Williams et al.,* 1996]. Obtaining this dependence from the formal considerations is a separate problem. The Earth is usually supposed to be perfectly conducting, while the ionosphere is characterized by an effective height and surface impedance [*Wait,* 1962; *Galejs,* 1972]. Rigorous but much more complicated approaches could be used [see *Makarov et al.,* 1994]. We apply the following heuristic dependence: $\nu(f) = \nu_1 - i\nu_2 = (f-2)/6 - if/100$ where f is measured in Hz. This dependence is based on statistical analyses of the SR cross-spectra obtained at two widely separated observatories [*Bliokh et al.,* 1980] and had been applied for modeling the ELF fields [*Nickolaenko,* 1995].

3. ELF Spectra

When computing the fields, we divide the frequency range into three strips and use different representations for the Legendre functions within these strips. We apply the zonal harmonic series representations (ZHSR) in the band $f \leq 250\ Hz$:

$$\frac{-\pi P_\nu(-x)}{\sin \pi\nu} = \sum_{n=0}^{\infty} \frac{(2n+1)P_n(x)}{(n-\nu)(n+\nu+1)} \qquad (3)$$

$$\frac{-\pi P_\nu^1(-x)}{\sin \pi\nu} = \sum_{n=0}^{\infty} \frac{\nu(\nu+1)(2n+1)P_n(x)}{[(n-\nu)^2-1)][(n+\nu+1)^2-1)]} \qquad (4)$$

Convergence of the ZHSR was accelerated in computation procedure [see *Nickolaenko and Rabinowicz,* 1974; *Bliokh et al.,* 1980; *Jones and Burke,* 1990; *Nickolaenko,* 1997].

The "cosine" and "sine" asymptotic expansions were used for frequencies $250\ Hz < f \leq 1.7\ kHz$, and exponential asymptotics were used when $f > 1.7\ kHz$. These last do not describe the characteristic amplitude oscillations of the field with the distance when an observer approaches the source antipode. Antipodal effect becomes pronounced in a close (500 - 1000 km) vicinity of the antipode because the attenuation of the radio waves is high.

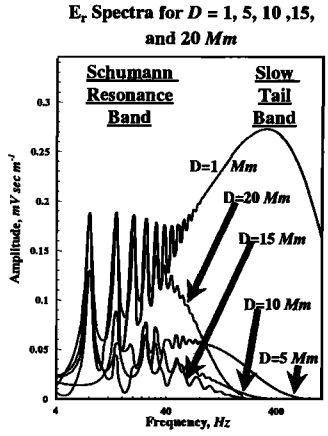

Figure 1. Samples of the wide–band $E_r(f)$ spectra for the source–observer distances $D = 1, 5, 10, 15$, and 20 Mm.

Fig. 1 presents the samples of the amplitude spectra for the source-observer distances D =1, 5, 10, 15, and 20 Mm. Frequency varying from 4 to 1000 Hz is plotted along the abscissa on a logarithmic scale. Amplitude of the electric field is shown along the ordinate in $mV\ sec\ m^{-1}$. The SR peaks are seen at the low frequencies $f < 100\ Hz$. Particular form of the resonance spectrum depends on the interaction between the direct (source-observer) and antipodal waves and this pattern is used for establishing the source-observer distance (SOD) for the ELF transient events or Q-bursts [*Kemp and Jones,* 1971; *Kemp,* 1971; *Burke and Jones,* 1992; *Nickolaenko and Kudinsteva,* 1994; *Sentman,* 1995a].

A broad spectral maximum occupies frequencies of some hundreds Hz when the SOD does not exceed a few thousands km. This is the frequency range of the slow tail atmospherics. As the distance increases, the peak decays due to absorption in the ionosphere that grows with frequency.

Fig. 2 depicts two contour maps showing the frequency-space distribution of the field amplitude. One may watch how the green hills and blue nodal zones drift toward the source antipode when the frequency increases. The feature is readily understood when we recall that the argument in the asymptotic field representation is of the form: $(\nu + 1/2)(\pi - \theta) - \pi/4$. It is easy to see that a particular element of the relief, say, a nodal zone occupies a hyperbolic area in the frequency–distance plane.

The peak-to-depression structures of the electric and magnetic fields have much in common:

(i) Both the fields contain the broad slow tail peak when the SOD is small;

(ii) There is "a one mode shift" present in the maps: the peaks of the horizontal magnetic field correspond to the nodes of the vertical electric field for the same SR mode number;

(iii) A succession of equidistant nodes and peaks is seen at the 10 Mm distance. Here, the odd modes are absent in the vertical electric field component and the even peaks disappear in the magnetic field;

(iv) A tendency to the antipodal effect becomes clear at higher frequencies, where a series of depressions extends itself toward the source antipode.

Schumann resonance and antipodal effects are well known [*Bliokh et al.,* 1980; *Kemp and Jones,* 1971; *Sentman,* 1995a, b]. Fig. 2 summarizes the individual wide-band plots in a compact way, revealing the features unseen in the separate plots of Fig.1.

The ELF field distribution in the frequency-distance domain demonstrates that the Q-bursts and slow-tail atmospherics are essentially the same phenomenon. The only difference lies in the source-observer distance. When SOD is small, the signal is concentrated over the higher frequencies, and the slow-tail waveform may be ob-

served. With the growth of SOD, the high frequency components attenuate, and the same pulse becomes a Q-burst having the energy centered in the SR band.

4. ELF pulse in the time domain

We obtained the waveforms after applying the FFT procedure to the spectral data. Fig. 3 depicts the $E_r(t)$ signal at 1, 5, 10, 15, and 20 Mm distance. Time in ms is plotted along the abscissa with $t = 0$ being the moment of the delta-discharge at the source. The arrows show the direct and antipodal waves in the figure. The direct wave arrives with a delay proportional to the SOD. Its amplitude is large at small SOD, and the pulse itself is short. When the distance grows, the waveguide works as a low-pass filter and the higher frequencies attenuate rapidly. As a result, the direct wave decreases and the pulse width increases. The amplitude of antipodal pulse grows when the SOD increases (distance to the source antipode decreases). Direct and antipodal waves become equal and merge into one pulse at the source antipode $D = 20\ Mm$.

The "plane geometry" of the direct and antipode waves is demonstrated in Fig. 4. Here we show the 3-D plot and the contour map of the $E_r(t)$ field component above the delay-distance plane. We had changed the sign of the pulse to make the relief clearer. The pulse "bounces" from the source antipode as if it propagates only along two great circle arcs: the direct and the antipodal paths. The rest of the spherical cavity plays a "supporting" role.

Influence of the waveguide sphericity is revealed by the pulse amplitude. The range dependence of the pulse amplitude is a decaying line with the field enhancements around the source and the antipode due to geometrical focusing of the waves in the spherical cavity. The simplified distance dependencies including the classical narrow-band representation of the form $[\exp(-\nu_2\theta)]/\sqrt{\sin\theta}$ [see *Wait*, 1962, p.291 and *Galejs*, 1972, p.97] differ from the broad-band pulse amplitude. The reason is in the absorption of the higher frequencies along the propagation path.

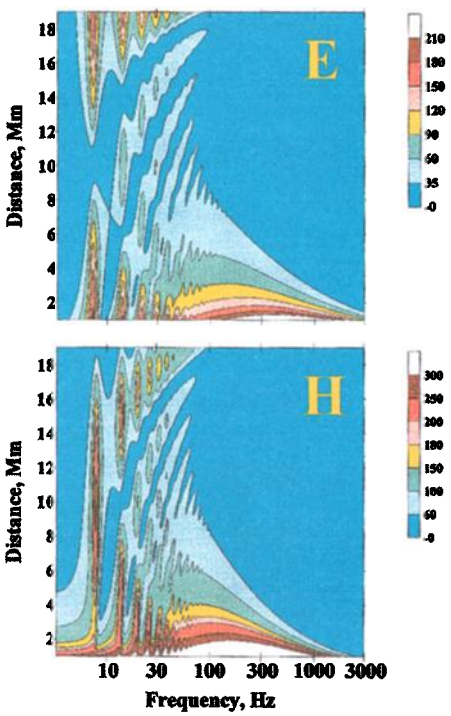

Figure 2. Contour maps of the amplitudes of the electric and magnetic fields over the frequency–distance plane. Peaks in the H_φ distribution correspond to the nodes of the vertical electric field. The nodal zones are seen as the blue strips approaching the source antipode.

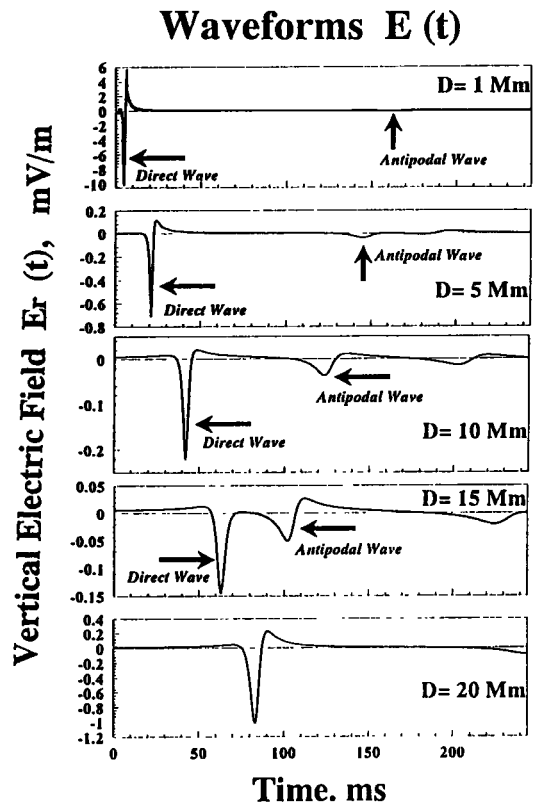

Figure 3. Waveforms of the vertical electric field at 1, 5, 15, and 20 Mm distance from the delta–pulse source.

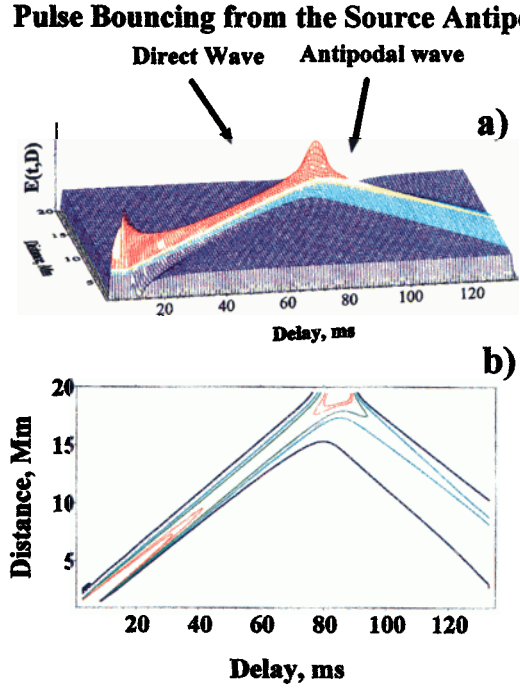

Figure 4. A 3-D view and a contour map of the ELF pulse "reflected" from the source antipode.

5. Conclusion

We had computed the fields from the point delta-source. Evolution of the fields occurred due to properties of the waveguide. The waveforms obtained have no quasi-periodic tails. To obtain such a tail, one should apply an enhanced radiation around some hundreds hertz frequency. Such a radiation compensates for the wave attenuation. For example, to provide the slow-tail demonstrated by *Reising et al.* [1996] one has to compensate for approximately 30 dB attenuation of the 200 Hz frequency at the 12 Mm distance. Therefore, the current moment of the source must involve a peak around this frequency due to continuing current of the stroke. The particular spectrum of the source is estimated from a ratio of the recorded pulse spectrum and the spectra computed for the same SOD.

To conclude the paper we repeat the main results.

1. The slow-tail atmospherics and the Q-bursts are essentially the same signals. The maximum of the EM power occupies the frequency of some hundreds hertz when the source-observer distance is a few Mm long. This explains an effectiveness of the nearby source location using the slow-tail atmospherics. From some Mm distance, the "high frequency" component vanishes, the electromagnetic energy is found in the SR band, and the signal transforms into a Q-burst. The global location of the lightning is possible at the frequencies below $80 - 100Hz$, where the radio wave attenuation in the Earth-ionosphere waveguide is relatively small.

2. The relief of the natural pulse signal over the frequency–distance plane has regular ridges, peaks and depressions. These structures are extended over hyperbolic lines in the frequency–distance plane. The relevant zones become straight over the distance–period plane.

3. The radio pulse moves with a constant velocity in the time domain. Its width grows monotonically with the propagation distance. A bouncing occurs from the source antipode.

4. The distance dependence of the wide-band pulse amplitude is governed by two factors. The first one is the field focusing around the source and its antipode in the spherical guiding system. The second factor is the ionospheric absorption. Attenuation of the higher frequencies modifies the pulse waveform, therefore the classical narrow-band field dependence does not describe the pulse amplitude versus propagation distance.

References

Bliokh, P.V., A.P. Nickolaenko, and Yu.F. Filippov, *Schumann resonances in the Earth–ionosphere cavity,* D.Ll. Jones–ed., Peter Perigrinus, Oxford, New York, Paris, 1980.

Boccippio, D.J., E.R. Williams, W.A. Lyons, I. Baker, and R. Boldi, Sprites, ELF transients and positive ground strokes, *Science*, 269, 1088-1091, 1995.

Burke, C.P., and D. Ll. Jones, An experimental investigation of ELF attenuation rates in the Earth-ionosphere duct, J. Atmos. Terr. Phys., *54,* 243-254, 1992.

Galejs, J., *Terrestrial propagation of long electromagnetic waves*, Pergamon Press, Oxford, New York, Paris 1972.

Hayakawa, M., K. Ohta and K. Baba, Wave characteristics of tweek atmospherics deduced from the direction finding measurement and theoretical interpretation, J. Geophys. Res., *99,* 10733-10743, 1994.

Jones, D. Ll. and C.P. Burke, Zonal harmonic series expansions of Legendre functions and associated Legendre functions, *J. Phys. A. Math. Gen.*, 23, 3159-3168, 1990.

Kemp, D.T., and D. Ll. Jones, A new technique for analysis of transient ELF electromagnetic disturbances within the Earth- ionosphere cavity, J. Atmos. Terr. Phys., *33,* 567-572, 1971.

Kemp, D.T., The global location of large lightning discharges from single station observations of ELF disturbances in the Earth- ionosphere cavity, J. Atmos. Terr. Phys., *33,* 919-928, 1971.

Lyons, W.A., Characteristics of luminous structures in the stratosphere above thunderstorm imaged by low-light video, Geophys. Res. Lett., *21,* 875-878, 1994.

Makarov, G.I., V.V. Novikov, and S.T. Rybachek, *Propagation of the radio waves in the Earth–ionosphere guiding system*, Moscow, Nauka, 1994, 152 pp.

Nickolaenko, A.P. and L.M. Rabinowicz, Speeding up the convergence of zonal harmonic series representation in the Schumann resonance problem, J. Atmos. Terr. Phys., *36,* 979-987, 1974.

Nickolaenko, A.P. and I.G. Kudintseva, A modified technique to locate the sources of ELF transient events, J. Atmos. Terr. Phys., *56,* 1493-1498, 1994.

Nickolaenko, A.P., ELF/VLF propagation measurements in the Atlantic during 1989, J. Atmos. Terr. Phys., *57,* 821-831, 1995.

Nickolaenko, A.P., Modern aspects of Schumann resonance studies, J. Atmos. Terr. Phys., *59,* 805-816, 1997.

Ogawa, T, Y. Tanaka, A.C. Fraser-Smith, and R. Gendrin, Worldwide simultaneity of a Q-burst in the Schumann resonance frequency range, *J. Geomagn. Geoelectr.*, 19, 377-384, 1967.

Reising, S.C., U.S. Inan, T.F. Bell, and W. A. Lyons, Evidence for continuing current in sprite producing cloud-to ground lightning discharges, Geophys. Res. Lett., *23,* 3639-3642, 1996.

Sentman, D.D. and E.M. Westcott, Observations of upper atmosphere optical flashes recorded from an aircraft, Geophys. Res. Lett., *20,* 2857-2860, 1993.

Sentman, D.D., E.M. Westcott, D.L. Osborne, D.L. Hampton, and M.J. Heavner, Preliminary results from the Sprites 94 aircraft campaign, Geophys. Res. Lett., *22,* 1205-1208, 1995.

Sentman, D.D., Schumann Resonances, *Handbook of atmospheric electrodynamics,* /H. Volland-ed. vol.1, Atmospheric electricity, 267-298, CRC Press Inc., Boca Raton, London, Tokyo, 1995a.

Sentman, D.D., Long baseline observations of Schumann resonance, Abstracts of reports at IUGG XXI General Assembly, Boulder, Colorado, July 2–14, 1995, MA22C-08, p.A280, 1995b.

Sukhorukov, A.I. and P. Stubbe, On ELF pulses from remote lightning triggering sprites, Geophys. Res. Lett., *24,* No.13, 1639-1642, 1997.

Wait, J.R. *Electromagnetic waves in stratified media,* Pergamon Press, Oxford, New York, Paris, 1962.

Williams, E., C. Wong, R. Boldi, and W. Lyons, Dual Schumann resonance methods for monitoring global lightning activity, Proc. 10th Int. Conf. on Atmospheric Electricity, Osaka, Japan, June 10–14, 1996, p 704–707, 1996.

M. Hayakawa and A. P. Nickolaenko Department of Electronic Engineering, The University of Electro-Communications, 1-5-1, Chofugaoka, Chofu-shi, Tokyo 182, Japan. (e-mail: sasha@whistler.ee.uec.ac.jp; hayakawa@whistler.ee.uec.ac.jp)

(Received January 26, 1998; revised April 27, 1998; accepted Apri 30, 1998.)